JOURNAL OF SOLID STATE CHEMISTRY 59, 280–290 (1985)

Host Lattice Dependence of the Bi^{3+} Luminescence in Orthoborates $LnBO_3$ (with Ln = Sc, Y, La, Gd, or Lu)

A. WOLFERT, E. W. J. L. OOMEN, AND G. BLASSE

Physical Laboratory, State University Utrecht, P.O. Box 80.000, 3508 TA Utrecht, The Netherlands

Received September 10, 1984; in revised form February 6, 1985

The luminescence properties of several Bi^{3+}-activated lanthanide borates ($LnBO_3$) are reported. For the calcite-structured borates ($ScBO_3$–Bi^{3+} and the high-temperature modification of $LuBO_3$–Bi^{3+}), the Stokes shift is small. In the luminescence spectra vibrational structure is observed. For the compounds with YBO_3 structure (low-temperature modification of $LuBO_3$–Bi^{3+} and YBO_3–Bi^{3+}) two luminescent centers are observed. Energy transfer occurs from one type of center to the other. Finally, for $LaBO_3$–Bi^{3+} two centers are also observed. One is ascribed to isolated Bi^{3+} ions and the other to Bi^{3+} pairs. The Stokes shift of the Bi^{3+} luminescence varies from 0.22 eV for $ScBO_3$–Bi^{3+} to 1.16 eV for $LaBO_3$–Bi^{3+}. This is discussed in terms of the increasing amount of space available to the Bi^{3+} ion in the host lattice.

1. Introduction

The luminescence properties of the Bi^{3+} ion depend strongly on the host lattice (*1–4*). In this report the luminescence of the Bi^{3+} ion in several lanthanide orthoborates ($LnBO_3$) is reported. Their luminescence at room temperature has been discussed by Blasse and Bril (*1*). In this study the measurements are extended to low temperatures. As far as possible, decay times were measured as a function of temperature.

The luminescence of the Bi^{3+} ion in $LiLnO_2$ and $NaLnO_2$ (with Ln = Sc, Y, La, Gd, or Lu) was studied in relation to the nature of the trivalent host lattice ions (*3*). In these systems the Bi^{3+} ion is octahedrally coordinated by oxygen ions. It appeared that the Stokes shift of the Bi^{3+} luminescence varies from 0.19 eV for $NaScO_2$–Bi^{3+} to 1.31 eV for $NaLaO_2$–Bi^{3+}. For samples with the smaller Stokes shift vibrational structure was also observed in the spectra.

For the orthoborates reported here, the crystal structure as well as the coordination of the trivalent cations are different. The compound $ScBO_3$ and a modification of $LuBO_3$ adopt the calcite structure (*5, 6*). In this structure the trivalent cation is octahedrally coordinated. Another modification of $LuBO_3$, and YBO_3 and $GdBO_3$, adopt the so-called YBO_3 structure (*7–9*). This structure is related to the vaterite structure. In this structure an octahedrally coordinated site and a 12-coordinated site is available for the trivalent ion in the ratio 2:1. For this 12-coordinated site, six oxygen neighbors are at a shorter and six others are at a longer distance. The last compound studied

0022-4596/85 $3.00

TABLE I

STRUCTURAL DATA OF THE HOST LATTICES STUDIED

Compound	Ionic radius of the Ln^{3+} ion (*10*)	Structure	Coordination of the Ln^{3+} ion
$ScBO_3$	0.745	Calcite	6
$LuBO_3$	0.861	Calcite	6
$LuBO_3$	0.861 (6 coord.)	YBO_3	6, 6 + 6
YBO_3	0.90 (6 coord.)	YBO_3	6, 6 + 6
$GdBO_3$	0.938 (6 coord.)	YBO_3	6, 6 + 6
$LaBO_3$	1.20	Aragonite	9

in this series was $LaBO_3$. The compound $LaBO_3$ has the aragonite structure (*5*, *6*), in which the La^{3+} ion is coordinated by nine oxygen ions. The structural properties, together with the ionic radii of the lanthanide ions are collected in Table I. From this table it is seen that the coordination number of the trivalent ion increases with increasing radius of the cation.

2. Experimental

Sample Preparation. Starting materials were: Sc_2O_3, Y_2O_3, Gd_2O_3 (Highways International, 99.99%), Lu_2O_3, La_2O_3 (Highways International, 99.999%), Bi_2O_3 ("Baker Analyzed"), and H_3BO_3 (Merck, pro analyse). The first step in the preparation of the Bi^{3+}-doped orthoborates was the preparation of $Ln_{2(1-x)}Bi_{2x}O_3$. Ln_2O_3 and Bi_2O_3 were dissolved in hydrochloric acid (Baker, 36%, pro analyse) and precipitated with ammonia (Merck, 25%, pro analyse). The precipitate was washed, dried, and fired in air at a temperature of about 500°C to convert the hydroxide into oxide. The preparation of the orthoborates then involves the reaction between $Ln_{2(1-x)}Bi_{2x}O_3$ and H_3BO_3. The oxide is mixed with hydroboric acid (excess 15%). This mixture is fired in air in a platinum crucible. The temperatures and firing times were different from each of the different compounds (see Table II).

The samples were checked by X-ray powder diffraction using $CuK\alpha$ radiation. The Bi^{3+} concentration in the different samples was determined by atomic absorption spectrometry.

Instrumentation. The luminescence spectra were recorded using a Perkin–Elmer MPF-3A spectrofluorometer, equipped with an Oxford-CF100 helium-flow cryostat. The excitation spectra were corrected for lamp intensity with the use of lumogen T-rot GG as a standard. The emission spectra were corrected for the photomultiplier sensitivity. The photon flux per constant energy interval Φ is obtained by multiplying the radiant power per constant wavelength interval by λ^3. The emission spectra with vibrational structure were recorded on equipment with a higher spectral resolution (~0.2 nm) [Ref. (*3*)]. The powders were mounted in an Oxford Instruments CF204 helium-flow cryostat. The excitation source was a 450-W high-pressure xenon lamp. The emission and excitation wavelengths were selected with a Leiss double and single monochromator, respectively. The emission was detected using a RCA C31034 photomultiplier.

The decay time measurements were performed with the use of an EG&G photon-counting system described in detail elsewhere (*4*). The excitation source consisted of an EG&G 108 AU xenon flash lamp (pulse width ~1 μsec).

TABLE II

FIRING TEMPERATURES AND TIMES FOR SOME RARE EARTH ORTHOBORATES

		Firing times in hours at			
Compound	Structure	400°C	700°C	1100°C	1200°C
$ScBO_3$	Calcite	1½	4	1½	—
$LuBO_3$	Calcite	1	3	—	2
$LuBO_3$	YBO_3	1	2½	—	—
YBO_3	YBO_3	1½	5	2	—
$GdBO_3$	YBO_3	1	3	3	—
$LaBO_3$	Aragonite	1	2½	—	—

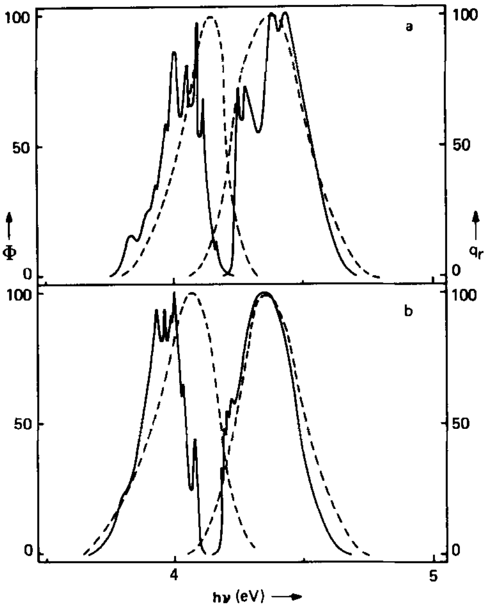

FIG. 1. Emission and excitation spectra of the luminescence of (a) $ScBO_3$–Bi^{3+} (0.12 a/o) and (b) $LuBO_3$–Bi^{3+} (0.13 a/o) at 4.2 K (—) and at 300 K (---). Φ denotes the radiant power per constant energy interval in arbitrary units. q_r specifies the relative quantum output in arbitrary units.

3. Results

3.1. Spectra

3.1.1. Compositions with the calcite structure ($ScBO_3$–Bi^{3+} and $LuBO_3$–Bi^{3+} [high-temperature modification]). The system $ScBO_3$–Bi^{3+} as well as $LuBO_3$–Bi^{3+} show efficient luminescence at 4.2 K. The emission and excitation spectra of $ScBO_3$–Bi^{3+} (0.12 a/o) at 4.2 and 300 K are shown in Fig. 1a. At 4.2 K vibrational structure is observed in the emission and excitation spectrum. The first line in the emission spectrum is at 4.16 eV and has low intensity. The excitation spectrum is split into two components, with double maxima, at 4.26 and 4.41 eV. At 300 K the maximum of the emission band is at 4.14 eV and the maximum of the excitation band is at 4.38 eV. The $Sc_{1-x}Bi_xBO_3$ compositions appeared to be single-phase up to a few percents in x. Concentration quenching of the Bi^{3+} emission occurred at a critical concentration (x_c) of about 1 a/o. The value of x_c is lower at 300 K than at 4.2 K.

The luminescence spectra of $LuBO_3$–Bi (0.13 a/o; calcite structure) are given in Fig. 1b. There is a resemblance with the luminescence spectra of $ScBO_3$–Bi^{3+}. At 4.2 K vibrational structure is observed in the emission spectrum and in the excitation spectrum. The vibronic structure is less pronounced than in $ScBO_3$–Bi^{3+} and the vibronic pattern is different. The first line in the emission spectrum is at 4.08 eV; it has a much higher intensity than that of the first line in the emission spectrum of $ScBO_3$–Bi^{3+}. The maximum of the emission band is at 4.08 eV at 300 K. The excitation spectrum consists of one band with a maximum at 4.35 eV. Only some weak vibronic lines are observed at 4.2 K. The line with the lowest energy is encountered at 4.18 eV. As in the case for $ScBO_3$–Bi^{3+}, concentration quenching of the Bi^{3+} emission is also observed for $LuBO_3$–Bi^{3+}. The critical concentration (x_c) is also 1 a/o at 4.2 K.

3.1.2. YBO_3-structured compounds (low-temperature modification of $LuBO_3$–Bi^{3+} and YBO_3–Bi^{3+} and $GdBO_3$–Bi^{3+}). The excitation and emission spectra of the low-temperature modification of $LuBO_3$–Bi^{3+} (0.3 a/o) are given in Fig. 2a. Two excitation bands and two emission bands are observed. The excitation bands are at 4.74 and 4.29 eV. Upon excitation at 4.29 eV one emission band, at 3.74 eV is seen (at 7 K). The emission band shifts to 3.76 eV at 300 K, this luminescent center will be called the L center. Upon excitation at 4.74 eV two emission bands are noted at 7 K. One emission band occurs at 3.74 eV and the other band, at 4.16 eV. The former is identical to the emission band observed upon excitation at 4.29 eV. At higher temperatures the intensity of the 4.16-eV emission band decreases, which makes it difficult to determine the position of this band

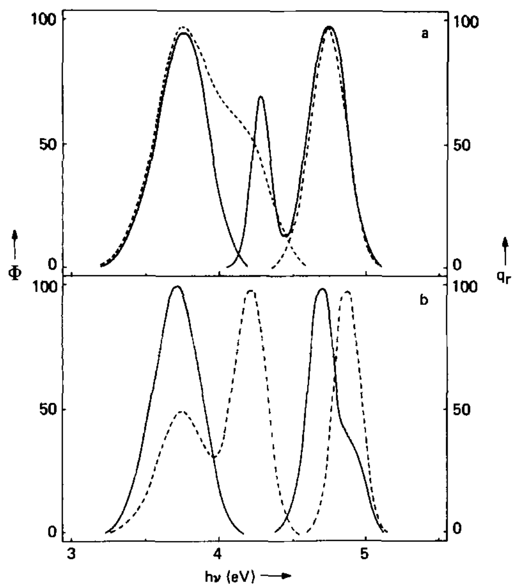

FIG. 2. Emission and excitation spectra at 7 K of the luminescence of: (a) $LuBO_3$–Bi^{3+} (0.3 a/o), emission spectrum (—) recorded for excitation at 4.29 eV, excitation spectrum (—) recorded for emission at 3.74 eV, emission spectrum (---) recorded for excitation at 4.74 eV, and excitation spectrum (---) recorded for emission at 4.16 eV. (b) YBO_3–Bi^{3+} (0.5 a/o), emission spectrum (—) recorded for excitation at 4.60 eV, excitation spectrum (—) recorded for emission at 3.72 eV, emission spectrum (---) recorded for excitation at 5.00 eV, and excitation spectrum recorded for emission at 4.20 eV.

at 300 K. A slight shift to higher energy is seen on going from 7 to 300 K. This center with its excitation at 4.74 eV and its emission at 4.16 eV will be called the H center. Excitation into the H center yields emission from the H center and from the L center. This is ascribed to energy transfer from the H center to the L center, which is observed down to low temperatures and down to low Bi^{3+} concentration (0.1 a/o).

Similar observations were made for YBO_3–Bi^{3+} (0.5 a/o). Two excitation bands are observed, one at 4.86 eV and the other at 4.70 eV at 7 K (Fig. 2b). Upon excitation at 4.70 eV one emission band, at 3.72 eV is seen. Increasing the temperature from 7 to 300 K makes the emission shift to 3.74 eV. This luminescent center will be called the L center. Excitation at 4.86 eV yields the emission band at 3.72 eV and an emission band at 4.20 eV. At 300 K this emission band is shifted to 4.22 eV but, just as in $LuBO_3$–Bi^{3+}, it is hard to determine the exact position. Similar to $LuBO_3$–Bi^{3+}, the center with its excitation at 4.86 eV and emission at 4.20 eV is called the H center. Energy transfer from the H center to the L center is encountered, whose efficiency depends on the Bi^{3+} concentration. In Fig. 3 the emission spectra upon excitation in the H center are shown for three different samples. To provide a comparison of these spectra they were normalized to the 4.20-eV emission. It is seen that for higher Bi^{3+} concentrations the energy transfer is enhanced. The energy transfer depends not only on the Bi^{3+} concentration, but also on temperature. This is shown in Fig. 4 for YBO_3–Bi^{3+} (0.5 a/o). At temperatures to 40 K about 70% of the emission occurs at 4.20 eV for excitation in the H center. Above 40 K the intensity of the 4.20-eV emission

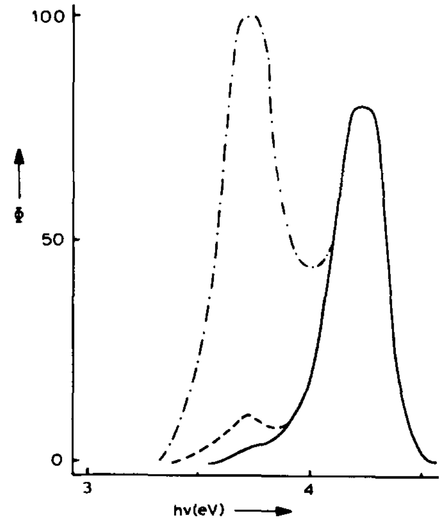

FIG. 3. Emission spectra of YBO_3–Bi^{3+} at 7 K for different Bi^{3+} concentrations (—) 0.5 a/o; (---) 1.0 a/o; and (-·-·) 2.5 a/o. Excitation energy: 5.00 eV.

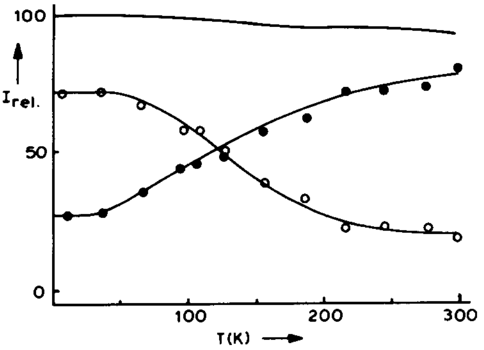

FIG. 4. Relative intensity of the 4.20-eV emission (○) and the 3.72-eV emission (●) of YBO_3–Bi^{3+} (0.5 a/o) as a function of temperature. Excitation energy: 5.00 eV. The total emission intensity is given by the upper line.

starts to decrease, while the intensity of the 3.72-eV emission increases. At about 120 K the intensities of both emissions are equal. At 300 K about 80% of the emission is due to the L center. The total intensity of the two emissions is almost constant in the temperature region of 4 K up till 300 K.

Remarkably enough the Bi^{3+} ion in $GdBO_3$ does not yield efficient luminescence, not even at 7 K. In view of our results for the isomorphous $LuBO_3$–Bi^{3+} (low-temperature modification) and YBO_3–Bi^{3+} the possibility that the Bi^{3+} emission in $GdBO_3$ is thermally quenched at 7 K can be excluded. The reason for the absence of Bi^{3+} emission in $GdBO_3$–Bi^{3+} is completely different, viz. energy transfer from Bi^{3+} to Gd^{3+} occurs. This has also been observed for GdB_3O_6–Bi^{3+} in which system it has been studied in detail (*11*, *12*).

What happens in $GdBO_3$–Bi^{3+} is most easily deduced from the excitation spectrum of the Eu^{3+} emission of this composition (Eu^{3+} is present as a starting impurity in Gd_2O_3). This spectrum is dominated by a Bi^{3+} excitation band in the short-wavelength UV region. In addition, the ^8S–^6P transitions of Gd^{3+} are observed, and, very weakly, some Eu^{3+} excitation lines. This shows that the excitation energy of the Bi^{3+} ion is transferred to the Gd^{3+} ion which transports the excitation energy through the lattice until it is trapped by suitable centers (Eu^{3+} for example) or emitted by the Gd^{3+} ions. For a more detailed description see (*12*). In addition to the Eu^{3+} emission we observed a broad band emission with a maximum at 2.80 eV. This is probably a Bi^{3+} defect center which acts as a trap. In view of the discussion below (Section 4.3) a Bi^{3+} pair center in low concentration is an obvious possibility. The results for $GdBO_3$–Bi^{3+} will not be discussed further.

3.1.3. Composition with the aragonite structure (*$LaBO_3$–Bi^{3+}*). At 7 K, two excitation bands and two emission bands are observed for $LaBO_3$–Bi^{3+} (0.08 a/o; Fig. 5). The excitation band at 4.62 eV is matched by an emission band at 3.46 eV; and the excitation band at 4.53 eV, by an emission band at 2.69 eV. The intensity of both emission bands is independent of temperature up to 300 K. The 3.46-eV emission band shifts to 3.51 eV at 300 K, while the position of the 2.69-eV emission band does not change for temperatures up to 300 K. No energy transfer from the 3.46-eV emitting center to the 2.69-eV emitting center is observed. For samples with a higher Bi^{3+} concentration an increase of the 2.69-eV emission relative to the 3.46-eV emission is encountered. This suggests that the 3.46-eV

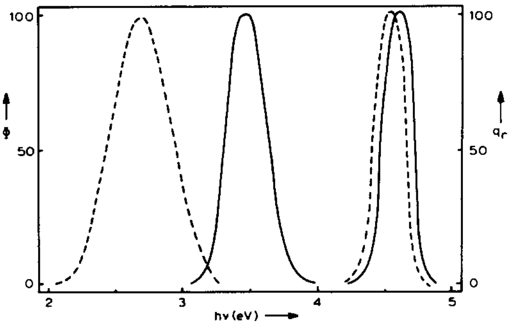

FIG. 5. Excitation and emission spectra of the luminescence of $LaBO_3$–Bi^{3+} (0.08 a/o) at 7 K. Full lines, isolated Bi^{3+}; broken lines, Bi^{3+} pairs.

TABLE III

SPECTRAL DATA OF THE Bi^{3+} LUMINESCENCE IN THE DIFFERENT LANTHANIDE ORTHOBORATES $LnBO_3$

Composition	Coordination	Excitation energy (eV)	Maximum emission energy at 7 K (eV)	Maximum emission energy at 300 K (eV)	Stokes shift[a] (eV)
$ScBO_3$–Bi^{3+}	6	4.26; 4.41 (4 K) 4.38 (300 K)	—	4.14	0.22
$LuBO_3$–Bi^{3+} (calcite)	6	4.35	—	4.08	0.28
$LuBO_3$–Bi^{3+}	6	4.74	4.16	~4.20	0.54
	6 + 6	4.29	3.74	3.76	0.53
YBO_3–Bi^{3+}	6	4.86	4.20	~4.22	0.64
	6 + 6	4.70	3.72	3.74	0.96
$LaBO_3$–Bi^{3+}	9 (Single)	4.62	3.46	3.51	1.16
	Pair	4.53	2.69	2.69	1.84

[a] Excitation energy-emission energy (at 300 K).

emission can be ascribed to isolated Bi^{3+} ions and the 2.69-eV emission, to Bi^{3+} pairs or to single Bi^{3+} clusters.

In Table III the positions of the excitation and emission bands of the compositions aforementioned are collected.

3.2. Decay Time Measurements

For only a few compositions, it was possible to determine the decay time of the emission as a function of temperature with the available setup. Of the calcite structured compounds, only the decay time of $ScBO_3$–Bi^{3+} (0.1 a/o) could be measured accurately as a function of temperature. Excitation occurred on the high-energy side of the excitation band. The decay curves were exponential. The decay time as a function of temperature, is given in Fig. 6. For $LuBO_3$–Bi^{3+} (calcite) only the low-temperature (4.2 K) decay time could be determined; it amounts to ~760 μsec. For $LaBO_3$–Bi^{3+} the decay time of both emissions was detected as a function of temperature (Fig. 7). The decay curves were exponential over the whole temperature region.

The decay times as a function of temperature were analyzed with the use of the well-known three-level scheme (*13, 14*) (see Fig. 8). Excitation occurs into level 2. After excitation two processes are possible: the radiative transition from level 2 to level 0, with probability k_{20}, and the nonradiative transition from level 2 to level 1 with probability k_{21}. If $k_{21} \gg k_{20}$, emission is observed

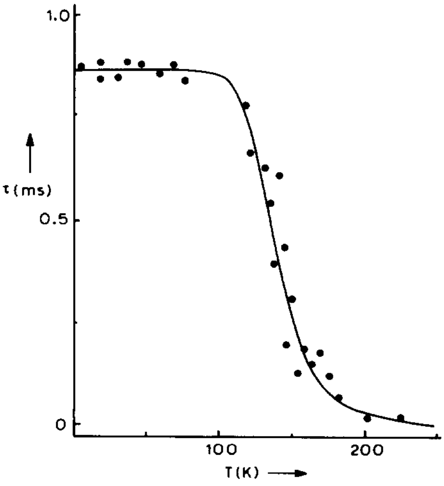

FIG. 6. Decay time of the 4.04-eV emission of $ScBO_3$–Bi^{3+} (0.12 a/o) as a function of temperature. The drawn line gives the best fit of the data to Eq. (2).

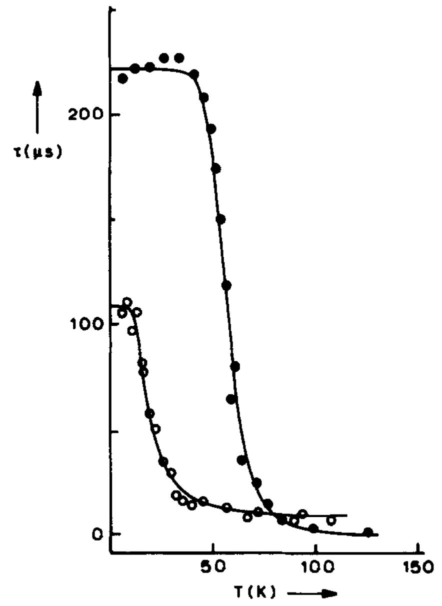

FIG. 7. Decay time of the 3.46-eV emission (●) and the 2.69-eV emission (○) of $LaBO_3$–Bi^{3+} (1 a/o) as a function of temperature. See also Fig. 6.

from level 1 at low temperatures; with a transition probability of k_{10}. The probability for the transition from level 1 to level 2 is given by

$$k_{12} = k_{21} \exp\left(\frac{-\Delta E}{kT}\right). \tag{1}$$

In Eq. (1), ΔE, denotes the energy difference between levels 1 and 2. At higher temperatures emission from level 2 can be observed. By assuming $k_{21} \gg k_{20}$ and $k_{20} \gg k_{10}$ the decay time of the total emission can be expressed as (*13, 14*)

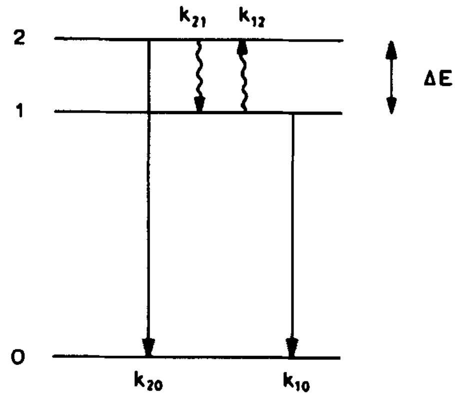

FIG. 8. The three-level scheme to analyze the decay time measurements. For explanation see text.

$$\frac{1}{\tau} = k_{10} + k_{20} \exp\left(\frac{-\Delta E}{kT}\right). \tag{2}$$

The value of k_{10} can be obtained from the low-temperature decay time ($k_{10} = \tau_0^{-1}$).

A fit of the experimental data to Eq. (2) yields k_{20} and ΔE. The results of the fit procedure for the different compositions are given in Table IV.

Discussion

4.1. Compositions with the Calcite Structure ($ScBO_3$–Bi^{3+} and High-Temperature Modification of $LuBO_3$–Bi^{3+})

The low-temperature emission bands observed for $ScBO_3$–Bi^{3+} and $LuBO_3$–Bi^{3+} (h*T*) can be ascribed to the $^3P_0$–$^1S_0$ transition. (Because the luminescence properties

TABLE IV

PARAMETERS DEDUCED FROM THE FIT TO EQ. (2) OF THE DECAY TIMES

Composition	Emission (eV)	Stokes shift (eV)	k_{10} (sec^{-1})	k_{20} (sec^{-1})	ΔE (meV)	Reference
$ScBO_3$–Bi^{3+} (0.12 a/o)	4.10	0.22	$(1.11 \pm 0.10) \times 10^3$	$(7 \pm 4) \times 10^7$	120 ± 2	This work
$LuBO_3$–Bi^{3+} (0.13 a/o)	4.08	0.28	$(1.31 \pm 0.10) \times 10^3$	—	—	This work
$LaBO_3$–Bi^{3+} (1 a/o)	3.46	1.16	$(4.55 \pm 0.06) \times 10^3$	$(2.5 \pm 1.0) \times 10^8$	55 ± 4	This work
$LaBO_3$–Bi^{3+} (1 a/o)	2.69	1.84	$(9.17 \pm 0.03) \times 10^3$	$(3.0 \pm 0.7) \times 10^5$	5.7 ± 0.4	This work
YOCl–Bi^{3+} (0.2 a/o)	3.00	1.87	$(9.26 \pm 0.03) \times 10^3$	$(7.5 \pm 0.4) \times 10^5$	4.9 ± 0.4	(*15*)

of the Bi^{3+} ion are reported for systems in which the site symmetry of the Bi^{3+} ion is different, we prefer the use of the free ion terms for the energy levels.) The low-temperature decay times are relatively large (Table IV) which agrees with the fact that this transition is forbidden. At higher temperatures the $^3P_1$ level becomes populated and emission is observed from this level: the emission bands shift to higher energy and the decay time decreases. The excitation bands are ascribed to the $^1S_0$–$^3P_1$ transition.

The site symmetry of the Sc^{3+} ion in $ScBO_3$ is S_6. This deviation from cubic symmetry is reflected in the excitation spectrum of the Bi^{3+} ion, where the $^1S_0$–$^3P_1$ transition is split by 0.15 eV due to the crystal field splitting of the $^3P_1$ level. The $^3P_1$ level splits, under S_6 symmetry, into a ^3E_u level and a ^3A_u level. In comparing the intensities of the two components of the excitation band, it can be assumed that the ^3A_u level is lower in energy than the ^3E_u level. For $LuBO_3$–Bi^{3+} the splitting of the excitation band is not observed. Due to the larger radius of the Lu^{3+} ion (see Table I), the crystal field at the trivalent ion site may be weaker in $LuBO_3$ than in $ScBO_3$. The difference in ionic radii results also in a difference between the Stokes shifts of the emissions of $ScBO_3$–Bi^{3+} and $LuBO_3$–Bi^{3+}. The Stokes shift of $LuBO_3$–Bi^{3+} is larger than that of $ScBO_3$–Bi^{3+}. The vibronic lines in the emission spectrum of $ScBO_3$ are rather pronounced. This indicates that in terms of a configurational coordinate diagram, the value of the parabolae off-set, Δr, is small, which results in a small Stokes shift. For $LuBO_3$–Bi^{3+} the vibronic structure is less pronounced, which indicates that the value of Δr is larger than in the case of $ScBO_3$–Bi^{3+}. As a consequence, the Stokes shift of $LuBO_3$–Bi^{3+} is also larger.

The energy difference between the first line in the emission spectrum and the first line in the excitation spectrum of $ScBO_3$–Bi^{3+} at 7 K is approximately 0.10 eV. From the decay time measurements the value of ΔE, the energy difference between levels 1 and 2 (Fig. 8), is 0.12 eV. In the case of $ScBO_3$–Bi^{3+} level 1 represents the $^3P_0$ state and level 2, the lower energy crystal field component of the $^3P_1$ state. The agreement of these two values of ΔE seems acceptable. This implies that the first line (4.16 eV) observed in the emission spectrum of $ScBO_3$–Bi^{3+} is the zero-phonon line. The relatively strong intensity of this line is due to the fact that the S_6 site symmetry does not forbid this transaction.

The occurrence of vibrational structure in the emission and excitation spectra of the Bi^{3+} ion has been observed several times before. Well-known examples are CaO–Bi^{3+} and MgO–Bi^{3+} [Ref. (*13*)], MgS–Bi^{3+} [Ref. (*16*)], $NaScO_2$–Bi^{3+} [Ref. (*3*)], and Cs_2NaYCl_6–Bi^{3+} [Ref. (*17*)]. Vibrational structure is observed if the Bi^{3+} ion is octahedrally coordinated and is substituted for a smaller ion (*3*). For Cs_2NaYCl_6–Bi^{3+} and $NaScO_2$–Bi^{3+} the vibrational structure was analyzed in terms of vibrations of the isolated BiO_6^{9-} or $BiCl_6^{3-}$ octahedron. In Cs_2NaYCl_6–Bi^{3+} the trivalent ion is octahedrally coordinated by chloride ions. These YCl_6^{3-} octahedra are isolated from each other by the sodium ions. Thus the YCl_6^{3-} octahedron (and also the $BiCl_6^{3-}$ octahedron) could be treated as an isolated unit. For the calcite-structured orthoborates $ScBo_3$–Bi^{3+} and $LuBO_3$–Bi^{3+} the situation appears to be more complicated.

For $ScBO_3$–Bi^{3+} the vibronic structure in the emission spectrum can be analyzed by taking into account only the Bi–O vibrations of the BiO_6^{9-} octahedron. In view of the agreement between the ΔE values derived from the spectra and the decay time measurements, it is assumed that the first weak line in the emission spectrum is the zero-phonon line. The other lines are assigned as follows: 400 ν_c, 650 $\nu_c + \nu_b$, 950 $\nu_c + \nu_a$, 1400 $\nu_c + 2\nu_a$, 1670 $\nu_c + 2\nu_a + \nu_b$, 1920

TABLE V

ENERGY TRANSFER DATA FOR $ScBO_3$–Bi^{3+}

Energy transfer via	T (K)	Q_A (eV cm^2)	$S.O.$ (eV^{-1})	R_c (Å)	x_c (a/o)
$^3P_0$	7	2×10^{-22}	2×10^{-2}	2.1	1500
$^3P_1$	300	1×10^{-17}	0.9	24	1.0

$\nu_c + 3\nu_a$. Here, the figure indicates the energy difference (cm^{-1}) between the vibronic line involved and the zero-phonon origin. Further, the same notation is used as for $NaScO_2$–Bi^{3+} [Ref. (*3*)]. Only the assignment of the broader line on the low-energy side of the emission band cannot be carried out in this manner.

The vibronic structure in the emission spectrum of $LuBO_3$–Bi^{3+} also cannot be analyzed in the same way. We were able to make an assignment involving similar vibrational frequencies, but unfortunately the spectra contain only a few vibronic lines, so that this assignment is not convincing. More intriguing, however, is the difference between the emission spectra of $ScBO_3$–Bi^{3+} and $LuBO_3$–Bi^{3+}, which have the same crystal structure. This may indicate a different orientation of the borate groups relative to the Bi^{3+} ion.

Because of the small Stokes shift observed for $ScBO_3$–Bi^{3+} energy transfer between the Bi^{3+} ion in the lattice is possible. This has also been noticed in $YAl_3B_4O_{12}$–Bi^{3+} [Ref. (*18*)]. The transfer parameters were calculated as indicated in the literature (*18–20*). Results are given in Table V. In this table, Q_A presents the absorption cross section, $S.O.$ the spectral overlap between the emission band and the excitation band. The parameter R_c presents the critical distance, the distance at which the probability for energy transfer is equal to the probability of the optical transition. Finally, x_c is the critical concentration.

It is seen from this table that energy transfer at 7 K via the $^3P_0$ level cannot occur. The critical distance for this process is only 2.1 Å. Energy transfer via the $^3P_1$ level is an efficient process. For Bi^{3+} concentrations >1 a/o concentration quenching is predicted to occur at 300 K, in agreement with experimental observation. This process will also be effective at 7 K, but x_c and R_c may not be calculated in this way, since we have neglected the nonradiative $^3P_1$–$^3P_0$ transition. At low temperatures this will decrease the $^3P_1$ population. Since at 7 K only $^3P_0$ emission is observed, the relevant nonradiative rate must be $\geq 10^2 \cdot k_2$. The transfer rate has to compete with this value, instead of with k_2. The occurrence of concentration quenching at 7 K shows that for certain distances the transfer rate does so successfully. A quantitative description seems to be difficult at this time.

4.2. Compositions with the YBO_3 Structure (Low-Temperature Modification (lT) of $LuBO_3$–Bi^{3+} and YBO_3–Bi^{3+})

For the compositions $LuBO_3$–Bi^{3+} (l*T*) and YBO_3–Bi^{3+} two luminescent centers are encountered, viz. one center emitting at high energy (the H center) and one emitting at lower energy (the L center). In the YBO_3 structure, two sites are available for the trivalent ions, a 6-coordinated site and a 6 + 6-coordinated site (see Introduction). In general the Bi^{3+} emission is at lower energy, if the coordination number or the space available for the Bi^{3+} ion increases (in fact these two parameters are not independent). In view of this the H center is assumed to be a Bi^{3+} ion at the 6-coordinated site, and the L center, a Bi^{3+} ion at the 6 + 6-coordinated site.

For $LuBO_3$–Bi^{3+} (l*T*), as well as for YBO_3–Bi^{3+}, the excitation bands can be ascribed to the $^1S_0$–$^3P_1$ transition, the low-temperature emission bands, to the $^3P_0$–$^1S_0$ transition and the emission bands at higher temperature, at slightly higher energy, to the $^3P_1$–$^1S_0$ transition.

The Stokes shifts of the emissions in $LuBO_3$–Bi^{3+} (l*T*) are about 0.54 eV for both

TABLE VI

DATA FOR THE ENERGY TRANSFER FROM THE H CENTER TO THE L CENTER IN $LuBO_3$–Bi^{3+} (1*T*) AND YBO_3–Bi^{3+}

Composition	*T* (K)	Q_A (eV cm²)	*S.O.* (eV⁻¹)	R_c Å
$LuBO_3$–Bi^{3+}	7	10^{-17}	5	30
YBO_3–Bi^{3+}	7	10^{-17}	10^{-2}	11

centers. For YBO_3–Bi^{3+}, the Stokes shifts are 0.64 and 0.96 eV for the H center and the L center, respectively. The Stokes shifts for $LuBO_3$–Bi^{3+} (1*T*) are smaller than for YBO_3–Bi^{3+}. This is in line with the general observation that the Stokes shift increases if the space available for the Bi^{3+} ion in the host lattice increases (*4*). This is also observed for the two different centers in YBO_3–Bi^{3+}, but, remarkably enough, not for the two centers in $LuBO_3$–Bi^{3+} (1*T*). Obviously, the relaxation process of the excited state responsible for the Stokes shift, in case of the L center in $LuBO_3$–Bi^{3+}, is mainly determined by the six nearby oxygen ions. The difference with the relaxation process in the H center is small. For the L center in YBO_3–Bi^{3+}, with a larger trivalent ion site, the influence of the six other oxygen ions, at a slightly larger distance is greater. This results in a difference of Stokes shift for the L center and the H center in YBO_3–Bi^{3+}.

As stated earlier, energy transfer from the H center to the L center is observed for both $LuBO_3$–Bi^{3+} and for YBO_3–Bi^{3+}. As mentioned above the critical distance R_c for energy transfer can be determined. Because decay time measurements of these systems are not available, we use for Q_A the value of 1×10^{-17} eV cm². The results for the two compositions are given in Table VI.

The table shows that in case of $LuBO_3$–Bi^{3+} energy transfer from the H center to the L center is a very efficient process at 7 K. The energy transfer process is less efficient for YBO_3–Bi^{3+} due to the smaller spectral overlap.

In Fig. 4 it can be seen that the efficiency of the energy transfer process in YBO_3–Bi^{3+} increases with increasing temperature. The energy transfer efficiency increases at temperatures above 40 K. The transfer process probably becomes more efficient as soon as the $^3P_1$ level becomes populated, because then the spectral overlap increases. This implies that the energy difference ΔE between the $^3P_0$ level and the $^3P_1$ level is smaller than in the case of $ScBO_3$–Bi^{3+}, which is in line with the empirical relation between the Stokes shift and ΔE (*21*). This relation states that for increasing Stokes shift the value of ΔE decreases. Because the Stokes shift of the emission in YBO_3–Bi^{3+} is larger than of the emission in $ScBO_3$–Bi^{3+}, the value of ΔE should be smaller in case of YBO_3–Bi^{3+}.

4.3. Composition with the Aragonite Structure ($LaBO_3$–Bi^{3+})

Despite the fact that in the aragonite structure only one crystallographic site is available for the trivalent ions, two luminescent centers are observed. As mentioned above (Section 3.1.3), the center with its emission at high energy is ascribed to an isolated Bi^{3+} ion, while the center with its emission at lower energy is ascribed to a Bi^{3+} pair or a simple Bi^{3+} cluster.

For the isolated Bi^{3+} ion the excitation band is ascribed to the $^1S_0 \rightarrow {}^3P_1$ transition. At low temperatures the emission can be ascribed to the forbidden $^3P_0 \rightarrow {}^1S_0$ transition (with a relatively long decay time, ~220 μsec). At higher temperatures the emission is ascribed to the partially allowed $^3P_1$–$^1S_0$ transition (with a short decay time, ~4 nsec). The energy difference between the $^3P_1$ level and the $^3P_0$ level amounts to roughly 6 meV. The Stokes shift of the emission is approximately 1.16 eV. The values fit reasonably to the empirical relation between the Stokes shift and ΔE (*21*). The Stokes shift of the emission from the isolated Bi^{3+} ion is large. The La^{3+} ion in $LaBO_3$ is coordinated by nine oxygen ions. The La–O distances vary from 2.40 to 2.74 Å [Ref. (*6*)]. Probably the Bi^{3+} ion in $LaBO_3$–Bi^{3+} is asymmetrically coordinated. Timmermans and Blasse showed that the Stokes shift of the Bi^{3+} emission is large (up to ~2 eV) if the Bi^{3+} ion is asymmetrically coordinated (*4*). The asymmetrical coordination of the Bi^{3+} ion in $LaBO_3$–Bi^{3+} is then responsible for the large Stokes shift.

The luminescence of the other center shows a remarkable resemblance to the luminescence of YOCl–Bi^{3+} (see Table IV). In YOCl–Bi^{3+} this luminescence was ascribed to Bi^{3+} pairs (*15*) which confirms our assignment. The occurrence of s^2 ion pairs is well known, e.g., Tl^+ in the alkali halides (*22*). Pairing of Bi^{3+} ions seems more favorable if the isolated Bi^{3+} ions show a large Stokes shift of their emission. This suggests that off-center Bi^{3+} ions may gain energy by occurring in pairs. Similar observations have been made for LaB_3O_6–Bi^{3+} (*12*).

5. Conclusions

The luminescence properties of the Bi^{3+} ion in the systems $ScBO_3$, $LuBO_3$, YBO_3, and $LaBO_3$ show a gradual variation which is best characterized by the increasing Stokes shift of the emission. This can be immediately correlated to the space available for the Bi^{3+} ion in the host lattice. If the available amount of space increases, the vibrational structure disappears and the Stokes shift increases. This forms a strong confirmation of the suggestion made earlier (*4*), that the Bi^{3+} ion tends to occupy an off-center position, which is only possible if enough space is available.

In addition, a number of efficient energy transfer phenomena have been observed in the orthoborates, viz. from Bi^{3+} to Gd^{3+} in $GdBO_3$–Bi^{3+}, from Bi^{3+} to Bi^{3+} on the same crystallographic sublattice in $ScBO_3$–Bi^{3+} and $LuBO_3$–Bi^{3+} (h*T*) and on different crystallographic sublattices in $LuBO_3$–Bi^{3+} (l*T*) and YBO_3–Bi^{3+}.

Acknowledgment

The authors are indebted to Mr. G. J. Dirksen for his assistance with the preparation of the orthoborates and for the performance of the atomic absorption analysis.

References

1. G. Blasse and A. Bril, *J. Chem. Phys.* **48,** 217 (1968).
2. G. Boulon, *J. Phys. (Paris)* **32,** 333 (1971).
3. A. C. van der Steen, J. J. P. van Hesteren, and A. P. Slok, *J. Electrochem. Soc.* **128,** 1327 (1981).
4. C. W. M. Timmermans and G. Blasse, *J. Solid State Chem.* **52,** 222 (1984).
5. R. W. G. Wyckoff, "Crystal Structures," Vol. II, Wiley, New York (1963).
6. R. E. Newnham, M. J., Redman, and R. P. Santoro, *J. Amer. Ceram. Soc.* **46,** 253 (1963).
7. W. F. Bradley, D. L. Graf, and A. S. Roth, *Acta Crystallogr.* **20,** 283 (1966).
8. J. P. Laperches and P. Tarte, *Spectrochim. Acta* **22,** 1201 (1966).
9. J. H. Denning and S. D. Ross, *Spectrochim. Acta Sect. A* **28,** 1775 (1972).
10. R. D. Shannon and C. T. Prewitt, *Acta Crystallogr. Sect. B* **25,** 925 (1969).
11. J. Th. W. de Hair and W. L. Konijnendijk, *J. Electrochem. Soc.* **127,** 161 (1980).
12. Hao Zhiran and G. Blasse, *Mater. Chem. Phys.* **12,** 257 (1985); *J. Lumin.* **31, 32,** 817 (1984).
13. A. E. Hughes and G. P. Pells, *Phys. Status Solidi B* **71,** 707 (1975).
14. G. Boulon, C. Pedrini, M. Guidoni, and Ch. Pannel, *J. Phys. (Paris)* **36,** 267 (1975).
15. A. Wolfert and G. Blasse, *Mater. Res. Bull.* **19,** 67 (1984).
16. S. Asano and N. Yamashita, *Phys. Status Solidi B* **105,** 305 (1981).
17. A. C. van der Steen, *Phys. Status Solidi B* **100,** 603 (1980).
18. F. Kellendonk, T. van den Belt, and G. Blasse, *J. Chem. Phys.* **76,** 1194 (1982).
19. D. L. Dexter, *J. Chem. Phys.* **21,** 836 (1953).
20. G. Blasse, *Philips Res. Rep.* **24,** 131 (1969).
21. G. Blasse and A. C. van der Steen, *Solid State Commun.* **31,** 993 (1979).
22. T. Tsuboi, *Phys. Rev. B* **29,** 1022 (1984).